# pH-Dependent Lytic Peptides Discovered by Phage Display†

Sachiko Hirosue‡ and Thomas Weber*,‡,§

*Department of Gene and Cell Medicine and Department of Cell, Molecular and Developmental Biology, Mount Sinai School of Medicine, New York, New York 10029*

*Received December 6, 2005; Revised Manuscript Received February 27, 2006*

ABSTRACT: Lipid membranes compartmentalize eukaryotic cells and separate the cell interior from the extracellular milieu. So far, studies of peptide and protein interactions with membranes have largely been limited to naturally occurring peptides or to sequences designed on the basis of structural information and biophysical parameters. To expand on these studies, utilizing a system with minimal assumptions, we used phage-display technology to identify 12 amino acid-long peptides that bind to liposomes at pH 5.0 but not at pH 7.5. Of the nineteen peptides discovered, three were able to cause leakage of liposome contents. Multivalent presentation of these membrane-active peptides by conjugation onto poly(L-Lysine) enhanced their lytic potential. The secondary structures were analyzed by circular dichroism in aqueous 2,2,2-trifluoroethanol and in buffered aqueous solutions, both in the presence and absence of liposomes. Two of the three lytic peptides show alpha helical profiles, whereas none of the nonlytic peptides formed stable secondary structures. The diverse characteristics of the peptides identified in this study demonstrate that phage-displayed peptide library screens on lipid membranes result in the discovery of nonclassical membrane-active peptides, whose study will provide novel insights into peptide−membrane interactions.

Membranes play an integral role in biology by acting as compartmentalizing barriers and are involved in many biological processes, such as signaling (*1*), membrane trafficking (*2*) including endo- and exocytosis (*3*), and viral cell entry and propagation (*4*).

Much of our understanding of protein−membrane interactions has been gained from studying the interaction of viral fusion proteins with membranes (*5*). The study of the interaction of fusion peptides of enveloped viruses with membranes proved to be particularly fruitful (*6*). The knowledge gained by these studies has not only greatly increased our understanding of the role of these fusion peptides in membrane fusion but also yielded important insights into the interaction of peptides with membranes in general. Furthermore, these studies allowed for the harnessing of peptides for improved delivery of genetic material and membrane-impermeable drugs into the cell cytoplasm (*7*).

Despite the large number of membrane-active peptides known, no apparent consensus sequence or motif exists that governs membrane activity (*8*). Mechanistically, membrane disturbance can range from surface or interfacial effects, such as the carpet model (*9*, *10*) membrane insertion (*11*), membrane fusion, pore formation, or membrane rupture. For each of these mechanisms, the structure and length requirements may be different. Until now, regions of both cellular and viral proteins as well as peptides that interact with membranes have been predominantly discovered by deletion and substitution studies (*12*), homology (*13*), photolabeling studies (*14*), and by biophysical analyses (*15*−*17*).

A more encompassing approach is an experimental one aimed at identifying peptides without being constrained by current paradigms. In this study, we achieve the identification of lytic peptides with minimal a priori assumptions. By using a phage-display peptide library screen (*18*) for peptides with membrane affinity, we circumvent structural or sequence restrictions used in rational peptide design (*19*, *20*) and avoid the limitations imposed by combinatorial chemistry (*21*). To test the concept, we have chosen to identify peptides that are lytic in a pH-dependent fashion. A deeper knowledge of pH-dependent lytic behavior will help us to understand better processes such as endosomal escape of viruses and gene delivery vehicles into the cytoplasm. The knowledge gained by these studies opens the possibility to develop methods in interfering with this step in the infectious pathway of pathological viruses. Furthermore, the insights gained will pave the way to increase endosomal escape of nonviral gene delivery vehicles.

## MATERIALS AND METHODS

*Materials.* The Ph.D.-12 phage-display Peptide Library Kit was purchased from New England Biolabs (Beverly, MA). All lipids were purchased from Avanti Polar Lipids (Alabaster, AL). *C*-terminally amidated peptides were either purchased as crude powder from Research Genetics (Invitrogen, Carlsbad, CA) with the exception of INF7*, which was purchased from Anaspec (San Jose, CA), or synthesized using the FastMocTM chemistry with Fmoc-Rink amide MBHA resin[1] (Anaspec, San Jose, CA) on an Applied Biosystems (Foster City, CA) 431A peptide synthesizer using the protocol of Fisher et al. (*22*). Cleavage from the resin

† This work was supported by a Basil O'Connor starter scholar research award from the March of Dimes Birth Defect Foundation (5-FY00−530 to T.W.) and a grant from the National Institute of Health (GM066313 to T.W.).

* To whom correspondence should be addressed. Tel: 212-659-8293. Fax: 212-849-2437. E-mail: thomas.weber@mssm.edu.

‡ Department of Gene and Cell Medicine.

§ Department of Cell, Molecular and Developmental Biology.

10.1021/bi052488s CCC: $33.50 
Published on Web 04/29/2006

and deprotection was accomplished with a mixture of trifluoroacetic acid (TFA)/phenol/water/thioanisol/1,2-ethanedithiol (EDT)/triisopropylsilane (TIPS) = 77.5:5:5:5:2.5:5. Peptide synthesis-grade reagents were purchased from Applied Biosystems, and the resin and protected amino acids were purchased from Anaspec (San Jose, CA).

Poly(L-Lysine) hydrobromide (pLLys) was purchased from Sigma (St. Louis, MO), catalog number P2636, Mw = 30−70 kDa. *N*-Succinimidyl 3-(2-pyridyldithio)propionate (SPDP) was purchased from Aldrich. Calcein (Sigma, St. Louis, MO) was used without further purification. All other chemicals were of reagent-grade unless otherwise noted.

*Preparation of Multilamellar Vesicles (MLV) for Library Screen*. Multilamellar vesicles were prepared either from 1-palmitoyl-2-oleoyl phosphatidylcholine (POPC) or from a mixture of lipids representing the endosomal membrane (endosomal lipid mix: ELM) (*23*). The endosomal lipid mix consists of liver PC/liver PE/brain PS/brain SM/cholesterol/liver PI/porcine brain ganglioside = 5:1:1:1:3:1:1. The lipid (1.5 $\mu$mol) was dried into a film under argon, and the residual solvents were removed under high vacuum for an hour. The lipid film was then dispersed in 500 $\mu$L of buffer (25 mM citric acid, 25 mM $Na_2HPO_4$, and 150 mM sodium chloride, adjusted to pH 5 with sodium hydroxide) with 10% fetal bovine serum (FBS, Mediatech, Herndon, VA). The serum was added in the buffer to mimic cell culture conditions. After vortexing for 4 min, the MLVs were collected by centrifugation for 4 min at 20 800*g* at 4 °C. The supernatant was removed, and the MLVs were resuspended in 500 $\mu$L of 10% FBS in pH 5 buffer for immediate use in screening experiments.

*Screening Procedure*. The screen was conducted as follows: $2.4 \times 10^{11}$ plaque-forming units (PFU) were diluted with pH 5 buffer with 10% FBS, which was added to prevent unspecific binding. To remove any traces of potential phage aggregates, the phage solution was centrifuged for 4 min at 20 800*g* at 4 °C. The supernatant was added to the MLVs to a final volume of 1 mL. After incubation for 15 min at 37 °C, with occasional shaking, those phages that bound to MLVs were harvested by collecting the MLVs by centrifugation for 4 min at 20 800*g* at 4 °C. The supernatant was removed by aspiration, and the pellet was resuspended in 1 mL of 10% FBS in pH 5 buffer. This washing procedure at pH 5 was repeated 10 times. After the final centrifugation, the MLV/phage pellet was resuspended in 1 mL of 10% FBS in pH 7.5 buffer (pH 7.5 buffer: 25 mM citric acid, 25 mM $Na_2HPO_4$, and 150 mM sodium chloride, adjusted to pH 7.5 with sodium hydroxide). Following a 15 min incubation at 37 °C, the phages that bound MLVs at pH 5 but were released from MLVs at pH 7.5 were harvested by removing the MLVs by centrifugation (10 min, 20 800*g*, 4 °C). This supernatant was transferred into a fresh tube for amplification. The amplification and titering steps were performed as described by the manufacturer. After four rounds of screening, the phages were harvested and plaques were picked for sequencing (Department of Human Genetics, Mount Sinai School of Medicine) using the primers provided in the kit.

*Peptide Purification*. The crude peptides were analyzed and purified on a Gilson HPLC system using reverse-phase Vydac Protein and Peptide C18 analytical and semipreparative columns (Grace Vydac, Hesperia, CA). The aqueous mobile phase consisted of 0.1% TFA or ammonium acetate in MilliQ water and the organic phase of 0.1% TFA or ammonium acetate in HPLC grade acetonitrile. The identity of the peptide was confirmed by MALDI-TOF (Rockefeller University, Protein DNA Technology Center, New York, NY).

*Conjugation of Peptide onto Poly(L-Lysine)*. Peptides were conjugated onto SPDP activated poly(L-Lysine) (pLLys) using a method described by Erbacher et al. (*24*). The fractions containing activated pLLys were then pooled and dialyzed against water. Activated pLLys was purified by gel permeation chromatography on a 1.25 × 45 cm Sephadex G25 column equilibrated in 0.15 M sodium chloride. The concentration of pLLys was determined by ninhydrin assay (*45*), and the grade of modification was measured by thiopyridone release at 343 nm after incubation with excess DTT.

Activated pLLys in one tenth of the total reaction volume (2.2 mL) was added dropwise to peptides dissolved in 5 × final reaction buffer (2 M guanidine hydrochloric acid, 20 mM ammonium bicarbonate), layered with argon, and rotated at room temperature overnight. The extent of reaction was analyzed by thiopyridone absorbance.

The peptide-pLLys conjugate was diluted 4-fold with 25 mM HEPES sodium hydroxide at pH 7.4 and purified by ion-exchange chromatography on a 1 mL HiPrep S column (equilibrated in 25 mM HEPES-sodium hydroxide at pH 7.4 and 0.5 M guanidine hydrochloric acid) using a linear gradient to 3 M guanidine hydrochloric acid. Elution profiles were monitored by ninhydrin assay (*45*). After dialysis against 25 mM HEPES-sodium hydroxide at pH 7.4 and 150 mM sodium chloride, the final concentration of pLLys-peptide conjugate was determined by ninhydrin assay (*45*). The final peptide concentration was determined by analytical HPLC after treatment with DTT and ninhydrin assay (*45*).

*Analysis of Peptide Binding to Multilamellar Liposomes*. Synthetic peptide (250 $\mu$M) was incubated with 2.5 mM MLVs of one of two lipid compositions in a total volume of 100 $\mu$L in either pH 5 or 7.5 buffer with 1 mM DTT. After incubation for 30 min at 37 °C, the peptide bound to liposomes was pelleted by centrifugation at 4 °C for 10 min at 20 800*g* followed by two washes with 200 $\mu$L of the respective chilled buffer. The pellets were dissolved in TFE and applied onto a thin-layer chromatography plate (Silica Gel 60 $F_{254}$, EMD Chemicals, Inc., Darmstadt, Germany). The peptide and lipids were resolved by thin-layer chromatography with the mobile phase (1-butanol/acetic acid/water = 5:2:3). The peptides were visualized by ninhydrin spraying (1 mg/mL ninhydrin in water-saturated *n*-butanol) and heating for color development.

[1] Abbreviations: CD, circular dichroism; ELM, endosomal lipid mix; EDT, 1,2-ethanedithiol; FBS, fetal bovine serum; LUVs, large unilamellar vesicles; MBHA resin, (4-(2′,4′-dimethoxyphenyl-Fmoc-aminomethyl-phenoxyacetamido-norleucyl)-4-methylbenzhydrylamine) resin; MLVs, multilamellar vesicles; POPC, 1-palmitoyl-2-oleoyl phosphatidylcholine; PBS, phosphate buffered saline; PC, phosphatidylcholine; PE, phosphatidylethanolamine; PI, phosphatidylinositol; 3H-DPPC, L-3−1,2-dipalmitoyl phosphatidyl [*N*-methyl-3H] choline; PS, phosphatidylserine; pLLys, poly(L-Lysine) hydrobromide; SUVs, small unilamellar vesicles; SM, sphingomyelin; SPDP, *N*-succinimidyl 3-(2-pyridyldithio)propionate; 2-TP, 2-thiopyridone; TCEP, tri(2-carboxyethyl)phosphine hydrochloride; TFA, trifluoroacetic acid; TFE, 2,2,2-trifluoroethanol; TIPS, triisopropylsilane; TX100, Triton X-100.

*Measurement of Leakage of Liposome Content*. Large unilamellar vesicles (LUVs) were prepared by extrusion using a Liposofast hand-held extruder ((*25*), Avestin, Ottawa, Canada) with 100 nm pore-sized polycarbonate filters (Avestin). Briefly, 25 $\mu$mol of lipid and 1 $\mu$Ci of L-1,2-dipalmitoyl, 3-phosphatidyl [*N*-methyl-$^3$H] choline ($^3$H-DPPC, Amersham Biosciences, Piscataway, NJ) in chloroform was dried into a film as described above. Liposomes for contents-leakage assays were prepared by hydrating the above film in 500 $\mu$L of calcein solution (40 mM calcein (neutralized with 3.75 equiv of sodium hydroxide) in pH 7.5 buffer) by vortexing. The lipid dispersion was then either sonicated to make SUVs (two-times-5 min continuous sonication in a water bath attachment at setting 10 with a Sonicator XL, Misonix, Farmingdale, NY) or extruded to make LUVs as described above. The free calcein was removed from liposomes by flotation on an Accudenz (Accurate Chemical & Scientific Corporation, Westbury, NY) density gradient. All Accudenz solutions are w/v in pH 7.5 buffer. The liposome solution (100 $\mu$L) was mixed with 100 $\mu$L of 40% Accudenz and introduced into 5 $\times$ 41 mm ultra-Clear ultracentrifuge tubes (Beckman Instruments, Palo Alto, CA). This solution was then overlaid in succession with 150 $\mu$L of 10%, 150 $\mu$L of 5%, and 100 $\mu$L of 0% Accudenz for POPC liposomes and 150 $\mu$L of 15%, 150 $\mu$L of 12.5%, 37.5 $\mu$L of 10%, and 100 $\mu$L of 5% Accudenz for ELM liposomes. The liposomes were centrifuged for 4 h at 4 °C at 48 000 rpm with the deceleration set at 5 on the Beckman L8-M ultracentrifuge in an SW55Ti swinging bucket rotor. The calcein-loaded POPC and ELM liposomes were isolated from the 0%/5% and 5%/10% interfaces, respectively. The lipid concentration was monitored by the amount of tritiated DPPC (Wallac 1409, Perkin-Elmer, Boston, MA; CytoScint, ICN, Costa Mesa, CA). Alternatively, the liposomes can be purified by repeated spin-column chromatography using Sephadex G25.

*Calcein Leakage Assay*. As originally described by Duzgunes et al. (*26*), contents leakage was measured by calcein release from the liposomes. Peptide stocks were made in DMF and borate buffer pH 8.4 mixtures to allow for complete dissolution of all peptides. Peptide concentrations were determined by a ninhydrin assay (*27*). The lipid concentrations are 25 $\mu$M unless otherwise noted. The final concentrations of stock components for leakage experiments were 1% DMF and 1.2 mM borate. The assays were conducted in 96-well plates (Nunc white polysorb plates, Nalgene Nunc International, Rochester, NY), and calcein fluorescence was followed in a fluorescence plate reader (fmax, Molecular Devices, Sunnyvale, CA). Excitation and emission wavelengths were set to 485 and 538 nm respectively. Fluorescence was measured in 1 min intervals with an integration time of 100 ms using SoftMax Pro 1.3.2 software. The reaction time was 30 min at 37 °C, after which complete leakage was determined by the addition of Triton X-100 to a final concentration of 0.25%.

*Calculation Method*. Percent leakage and leakage units were calculated as defined by Plank et al. (*28*).

*Calcein Leakage in the Presence of pLLys−Peptide Conjugates*. Calcein leakage studies conducted with peptide−pLLys conjugates were normalized for peptide concentration as determined above, with and without 1 mM DTT.

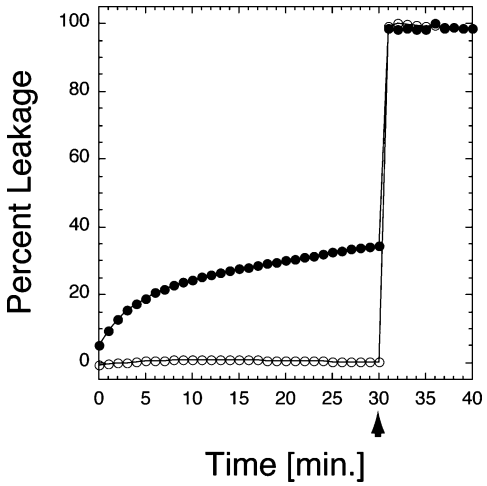


FIGURE 1: Lytic activity of PC1. A typical calcein release assay with PC1 is shown. The peptide was incubated at pH 5 and 7.5 in the presence of calcein-loaded phosphatidylcholine large, unilamellar vesicles approximately 100 nm in diameter (POPC LUVs). PC1 and lipid concentrations were 25 $\mu$M. The incubation temperature was 37 °C. Leakage was followed by measuring the increase in calcein fluorescence at 485/537 nm. At 30 min (arrowhead), TX100 was added to a final concentration of 0.25%. Percent leakage was calculated by setting the fluorescence of liposomes in buffer at time = 0 min as 0% leakage and fluorescence after complete lysis by TX100 addition as 100% leakage. Symbols: 25 $\mu$M PC1 at pH 5 (●); 25 $\mu$M PC1 at pH 7.5 (○).

*Circular Dichroism*. Peptide conformation was studied by circular dichroism (CD) spectroscopy using a JASCO J-810 CD spectrometer with a 1 mm path length quartz cuvette (Hellma QS 284, Hellma U.S.A., Plainview, NY). All spectra are averages of four measurements taken between 250 and 190 nm at 25 $\pm$ 2 °C, unless noted otherwise.

The peptide stock solutions were prepared in 2,2,2-trifluoroethanol (TFE). Measurements were performed in TFE/water = 1:1 with 1 mM TCEP. The pH of these solutions was 3.0. For measurements of peptides in aqueous solution, the peptides were dissolved in 0.1% ammonia from which dilutions were made. The final CD buffer was 0.01% ammonia, 2 mM citrate, 2 mM borate, and 2 mM potassium phosphate buffered with 10 mM sodium chloride and 10 mM TCEP. The buffering components were used to adjust the solutions to either pH 5 or 7.5. If present, the liposomes (SUVs), made as described above, were added to the peptide solution in less than 10% of the total volume. The peptide concentrations were derived from amino acid analysis (Rockefeller University Protein DNA Technology Center, New York, NY).

*Bioinformatics Analysis*. The probability that a peptide sequence occurred by chance, and positional amino acid frequencies were calculated using algorithms in RELIC: INFO and AAFREQ (which was modified so peptide redundancies were allowed) (*30*). The unamplified Ph.D.-12 library sequences were obtained from http://relic.bio.anl.gov/relicPeptides.aspx (file ran-12s.txt). Normalized amino acid occurrences for Figure 4 were calculated with these data, namely, the frequency of a residue found in our phage screen divided by that of the parent library. The probability that amino acid X occurs at position *y* by chance in *n* out of *N* picked phage clones was calculated as follows

$$(F_{\text{Ph.D.}-12}(\text{X at } y))^n \times (1-(F_{\text{Ph.D.}-12}(\text{X at } y)))^{(N-n)}$$

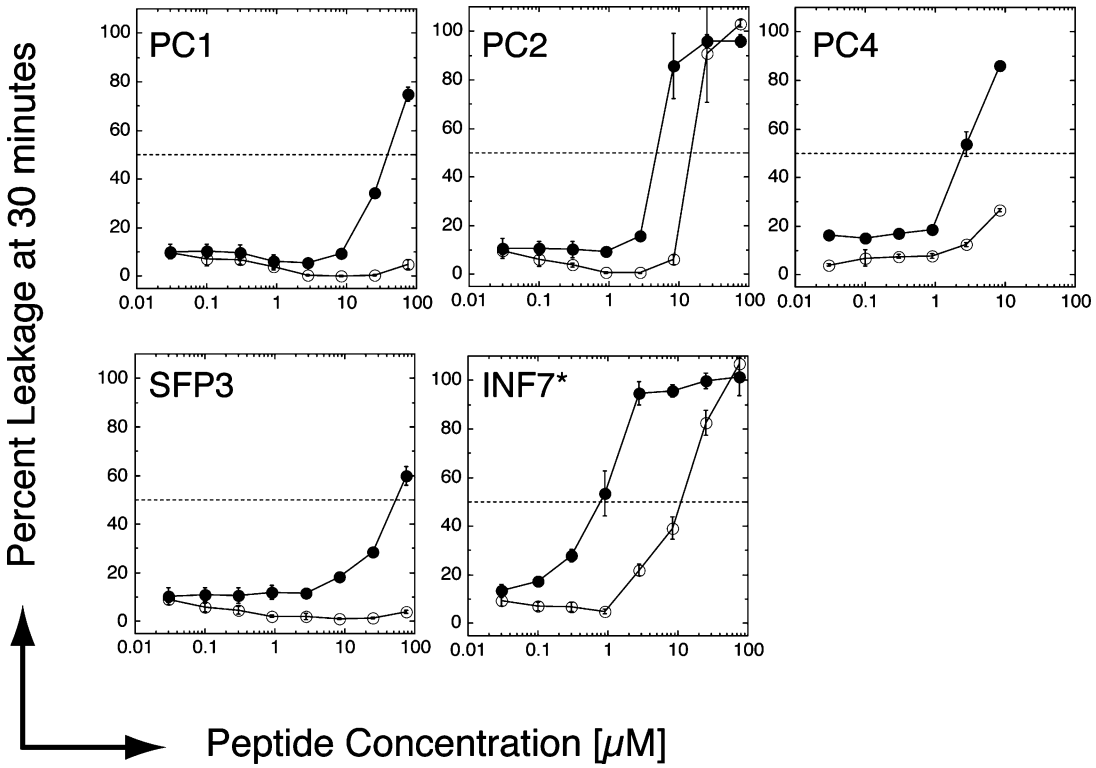


FIGURE 2: Extent of pH-dependent leakage of all peptides. Leakage studies were conducted as described for Figure 1 at various peptide concentrations (0 to 75 $\mu$M, except for PC4, for which the concentration range was 0 to 8.3 $\mu$M because of peptide aggregation in solution). The extent of leakage after 30 min of incubation with peptide was plotted against peptide concentration as an average of three independent experiments ± standard deviation. Symbols: pH 5 (●); pH 7.5 (○); 50% leakage (---).

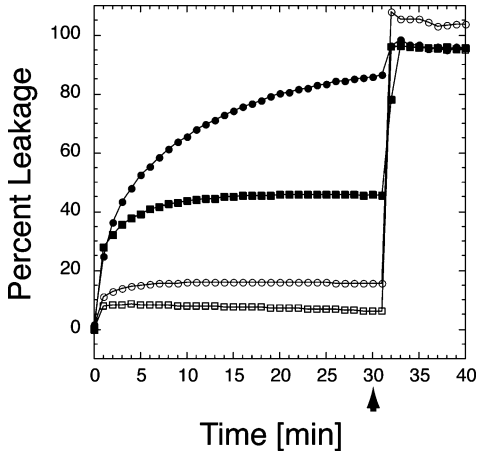


FIGURE 3: Effect of oligomeric presentation on pH-dependent contents leakage from liposomes. Calcein leakage in the presence of PC1−poly(L-Lysine) (pLLys) at 25 $\mu$M PC1 was followed as described for Figure 1. The peptides were coupled via their cysteine residues to the $\epsilon$-amino groups of 46 kDa pLLys at 16.6 ± 1.7%, as described in ref *24* and Materials and Methods. Symbols: conjugated peptides at pH 5 (●); free peptides (i.e., released from pLLys with 1 mM DTT) at pH 5 (■); conjugated peptides at pH 7.5 (○); free peptides at pH 7.5 (□). The arrowhead denotes the time of TX100 addition.

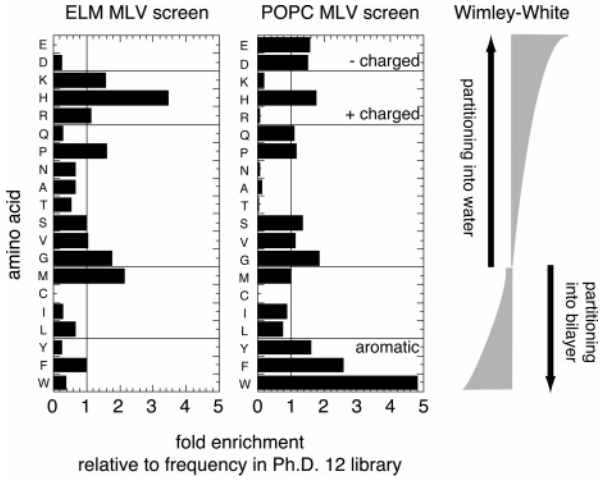


FIGURE 4: Amino acid occurrence in discovered peptides. The frequency of amino acids in the peptides discovered from the screen was normalized against that of the parent Ph.D.-12 library. The parent library's amino acid frequency has been previously determined and was calculated from the sequences of 100 randomly selected phage clones (see Materials and Methods and ref *39*). The amino acids are ordered according to the residue's propensity of partitioning into either water or liposomal bilayers. This rank order is depicted according to the Wimley−White water/bilayer whole residue hydrophobicity scale (*51*). Wimley−White obtained this scale by experimentally determining the free energy of transfer (kcal·mol$^{-1}$) of an amino acid residue from water into a POPC bilayer. Each peptide sequence that was isolated more than once was counted as a distinct peptide for each of the occurrences.

where $F_{\text{Ph.D.}-12}$(X at $y$) is the frequency of X at position $y$ found in the unamplified Ph.D.-12 library.

BLAST searches were done on NCBI BLAST (http://www.ncbi.nlm.nih.gov/BLAST/) for short, nearly exact matches. Significant motifs were not found within the discovered peptides according to MEME·MAST (http://meme.sdsc.edu/meme/website/intro.html) (*31*).

## RESULTS

*Phage Screen and Identified Peptides.* All viruses have to breach a cellular membrane to access the cytoplasm. Inevitably, this requires the interaction of viral proteins with

Table 1: Sequences of Peptides Identified after Four Rounds of Panning[a]

| Liposome Screened | Peptide | Sequence | Occurrence |
|---|---|---|---|
| **Phage Library Screen** | | | |
| PC | PC1 | **H W Y D S F V P W G H Q** C | 16 |
| | PC2 | **I P S P L E F L S E L M** C | 7 |
| | PC3 | **K M P I P S P A M P F G** C | 1 |
| | PC4 | **S S A W W S Y W P P V A** C | 1 |
| | PC5 | **L P L M K T N E Y P D L** C | 1 |
| | PC6 | **G Y F S P R I S P S P S** C | 1 |
| ELM | ELM1 | **M H G K V H H P L S P R** C | 5 |
| | ELM2 | **M G H S H N T P A P K S** C | 2 |
| | ELM3 | **G H F N K H M R A S V P** C | 2 |
| | | L T H H T S P P P V P A | 1 |
| | | M H H A P R L N P P V M | 1 |
| | | M H S H W Q R P Q S P F | 1 |
| | | M H H P V Y P F Q H P P | 1 |
| | | L T T H N T W F H H R S | 1 |
| | | L S H H K T V P I D A N | 1 |
| | | A H F G K P P H F G S S | 1 |
| | | M H R H L G P A L S D A | 1 |
| | | M H S P H R T L P I L T | 1 |
| | | Y H P R A L T P P T P L | 1 |
| **Positive Controls** | | | |
| | SFP3 | **W E A A L A E A L A E A L A C** | |
| | INF7* | **G L F E A I E G F I E N G W E G M I D G W Y G** C | |

[a] Two distinct lipid mixtures, POPC and ELM, were used in panning to screen for peptides with pH-dependent membrane-binding activity (Materials and Methods). Those peptides that were further characterized are in bold with an additional *C*-terminal cysteine that was used in conjugation studies. In addition, the sequence of positive control peptides INF7* and SFP3 are shown.

cellular membranes. These interactions can occur either at the plasma membrane (e.g., HIV (*32*)) or in the endosomal system (e.g., influenza (*33*) and adenovirus (*34*)). Conformational changes of both class I and class II fusion proteins of enveloped viruses (*35*) play an essential role in the fusion of viral and cellular membranes. It has been recognized early on that the pH-dependent interaction of fusion peptides with lipid bilayers are an important part of merging of membranes (*12*, *36*, *37*). That pH-dependent membrane interactions are also vital in the endosomal escape of nonenveloped viruses is demonstrated by the pH-dependent insertion of the capsid protein of rhinoviruses into the endosomal membrane (*38*). Because of our interest in finding regions of other nonenveloped viruses involved in endosomal escape, we set out to identify peptides that act on membranes in a pH-dependent manner.

Although different mechanisms can be envisaged that result in such pH-dependency, we reasoned that one possible basis for pH-dependent membrane activity is the ability of peptides to bind only to membranes at acidic but not at neutral pH. Thus, the screen was designed to identify peptides that bind to membranes at pH 5 but not at 7.5. Peptides with pH-dependent membrane binding properties were discovered by panning a phage-displayed peptide library against multilamellar vesicles (MLVs) at the two pH conditions. For our screening, the Ph.D.-12 library (NEB, Beverly, MA), which is composed of $2.7 \times 10^9$ random combinations of 12 amino acids, was used. The peptides in this library are linked by a GGGS spacer to the *N*-terminus of the minor coat protein pIII of the filamentous phage M-13. Specifically, the library of the filamentous phage was incubated with MLVs at pH 5. Phages that stably bind to MLVs were then isolated by collecting the MLVs by centrifugation; nonbinding phages remained in the supernatant. Those phages that did not firmly bind to MLVs at pH 7.5 were selected by eluting phages with pH 7.5 buffer at 37 °C. This eluant was amplified to repeat the panning three more times (Materials and Methods).

Two different lipid compositions were used in this screen to select for peptides that interact either with the aliphatic bilayer core (using electroneutral PC liposomes) or the polar headgroups of the endosomal membrane (using an acidic endosomal lipid mix (ELM) described in the literature (*23*)).

These experiments yielded 19 distinct peptide sequences, which are listed in Table 1. Some peptides occurred multiple times after four rounds of panning. This is not a result of the incomplete sequence representation, the positional amino acid biases dictated by M13 phage biology of the parent Ph.D.-12 library (*39*), or individual phage growth biases because the number of occurrences in the screen does not correlate with the probabilities of the sequences to occur randomly in the parent library (Supporting Information, Table 1).

*In Vitro Characterization of Peptides.* Overall, 11 short peptides were characterized for their ability to interact with and disturb membranes. Of the discovered peptides, all of

Table 2: Peptide Binding to Multilamellar Vescicles (MLVs)[a]

| | ELM MLV | | POPC MLV | |
|---|---|---|---|---|
| peptide | pH 5 | pH 7.5 | pH 5 | pH 7.5 |
| PC1 | + | + | + | + |
| PC2 | [b] | [b] | + | + |
| PC4 | [b] | [b] | + | + |

[a] Peptide binding was assessed by incubating 250 $\mu$M peptide with 2.5 mM MLVs in either pH 5 or 7.5 buffer for 30 min at 37 °C. After pelleting the MLVs by centrifugation, both the supernatant and pellet were analyzed for the presence of peptides by thin-layer chromatography (TLC) and visualization by ninhydrin staining. [b] The amino lipids in ELM MLVs could not be resolved from PC2 and PC4, making the analysis of binding of these peptides to ELM MLVs impossible.

Table 3: Summary of Leakage Activity of All Peptides[a]

| | leakage units ($\mu$L/$\mu$g) POPC LUVs | |
|---|---|---|
| peptide | pH 5 | pH 7.5 |
| PC1 | 13.6 ± 0.3 | [b] |
| PC2 | 122.4 ± 12.8 | 39.4 ± 5.2 |
| PC4 | 303.9 ± 118.2 | [b] |
| SFP3 | 11.0 ± 0.7 | [b] |
| INF7* | 435.6 ± 107.7 | 30.2 ± 4.3 |

[a] The leakage units were calculated from three independent samples as described in Plank et al. (*26*) and in Materials and Methods. The leakage units essentially represent a molar leakage coefficient corrected for peptide length. [b] Within the concentration range tested (0 to 75 $\mu$M, except for PC4, which was 0 to 8.3 $\mu$M because of peptide aggregation in solution), the peptides did not demonstrate 50% leakage after 30 min and, therefore, did not allow the calculation of leakage units.

the peptides recovered from the POPC MLV screen and the three peptides that occurred more than once in the ELM MLV screen were used. As positive controls for membrane activity, two peptides were chosen that are known to be membrane-active in a pH-dependent manner (Table 1). INF7 is the first 23 amino acids of the amino-terminal sequence of influenza virus X-31 (H3N2) hemagglutinin subunit HA-2 with two G to E substitutions (positions 4 and 7) that render the peptide more membrane-active in in vitro assays (*28*). The other peptide is a 15-mer known as short fusion peptide 3 (SFP3) (*40*). This amphipathic peptide is a shortened version of the synthetic pH-sensitive peptide GALA (*41*), which has been described in detail for its membrane activity in vitro (*20*). In addition to the relevant amino acid sequences, a cysteine was added to the *C*-terminus of each peptide (except for SFP3, which already has a *C*-terminal cysteine). Each peptide is named after the screen from which it was recovered. INF7 with the *C*-terminal Cysteine is now called INF7*. This additional cysteine allowed the conjugation of the peptides to poly-(lysine) for multimeric presentation as discussed later. The *C*-termini were amidated.

*MLV Binding of Free Peptides.* The 13-mer peptides were first tested to determine whether they retained the ability to bind to liposomes on which the screen was based. To demonstrate peptide association with MLVs, individual peptides were incubated with POPC or ELM MLVs under the same pH conditions as those for the phage screen. After centrifugation, the peptides and lipids in the pellet were separated by thin-layer chromatography and the peptides visualized by ninhydrin spray. For optimal recovery and detection, 250 $\mu$M peptide and 2.5 mM lipid were used. The peptides ELM1, ELM2, ELM3, PC3, PC5, and PC6 were, in contrast to PC1, PC2, and PC4, not detectable in the pellet of POPC MLVs (Table 2 and data not shown). For technical reasons, it was not possible to measure the binding of PC2 and PC4 to ELM MLVs. Of the remaining peptides, however, only PC1 could bind to ELM MLVs (Table 2). PC4 also pelleted in the absence of MLVs in a pH-independent manner, although to a lesser degree than in their presence, suggesting that PC4 has a tendency to aggregate under these conditions (data not shown).

*Contents-Leakage Assay.* To analyze the lytic potential of our peptides, the ability of these peptides to induce leakage of vesicle contents of large unilamellar liposomes (LUVs) was tested. To measure liposome leakage, a well-established contents-leakage assay (*26*) was used. In this assay, the fluorophore calcein is entrapped in the liposomes at self-quenching concentrations; when released into the surrounding buffer, quenching is relieved, resulting in increased fluorescence. A typical calcein release curve during incubation of 25 $\mu$M PC1 peptide with POPC LUVs at 37 °C can be seen in Figure 1. As expected, because of substrate (i.e., nonlysed, calcein filled liposomes) depletion, the leakage curve was biphasic. At pH 5, the initial release rate was 4.2% leakage/min, and the extent of leakage at 30 min was 34.5%. At pH 7.5, however, leakage was negligible.

To determine the relative leakage activity of each peptide, contents leakage was determined at peptide concentrations from 0 to 75 $\mu$M (except for PC4, for which the highest concentration was 8.3 $\mu$M because of peptide aggregation at higher concentrations). Whereas the peptide concentrations were varied as a 3-fold dilution series, the lipid concentration was kept constant at 25 $\mu$M. The titration curves for all the peptides analyzed by this method are shown in Figure 2. To summarize the leakage data from various concentrations of all peptides, their activity was represented in leakage units as previously defined by Plank et al. (Table 3) (*28*). Leakage units are defined as the inverse of the amount of peptide (expressed in $\mu$g) necessary to result in $\geq$50% leakage after 30 min (*28*). In effect, leakage units represent a molar leakage coefficient corrected for peptide length.

As anticipated, some peptides PC1, PC2, and PC4, namely, those which bound to MLVs, as well as the two positive control peptides SFP3 and INF7* demonstrate membrane activity with greater leakage at pH 5 than at 7.5 (Figure 2 and Table 3). The other peptides analyzed do not show any activity under these conditions (data not shown). The leakage triggered by INF7* is comparable to the results reported by Plank et al. (*28*) (Table 3). PC4 is almost as active as INF7*, whereas PC2 is approximately 3-fold less active. The leakage activities of SFP3 and PC1 at pH 5 are more than 1-order of magnitude lower than the activity of INF7* (Table 3, Figure 2). For certain peptides and pH conditions, it was not possible to calculate leakage units because 50% leakage was not reached in the concentration range tested. For two of these conditions, namely, PC1 and SFP3 at pH 7.5, the leakage was negligible. For the third condition, PC4 at pH 7.5, the leakage measured at the highest peptide concentration without detectable peptide aggregation reached 27% (Figure 2), approximately 3-fold lower than the leakage observed at pH 5.

The pH dependence is strongest for PC1, SPF3, and INF7*. The leakage observed with INF7* was approximately

15-times higher at pH 5 than at 7.5 (Table 3, Figure 2). The difference in leakage activity at pH 5 and 7.5 for PC2 is 3-fold (Table 3). The leakage for PC1 and SFP3 at pH 7.5 was negligible even at the highest concentrations tested (Figure 2). Similar results were obtained with calcein-loaded ELM liposomes.

*Oligomeric Presentation of Peptides.* Because most fusion or lytic peptides of enveloped and nonenveloped viruses are presented as part of a protein, often in multimeric form (*42*), we tested the effect of oligomeric presentation of the membrane-active peptides PC1, PC2, and PC4. Using SPDP chemistry, the peptides were coupled to poly (L-Lysine) (pLLys) (Mw = 30−70 kDa) via a disulfide bond from their *C*-terminal cysteines to modified $\epsilon$-amino groups of the lysines. With this procedure, 16.6 ± 1.7% of all lysines were carrying a peptide. The conjugates were then incubated with POPC liposomes in the presence or absence of DTT. In other words, the peptides were either released from pLLys by reduction of the disulfide bridge in the presence of DTT or remained conjugated in the absence of DTT. Analysis in the leakage assay showed that the conjugated form of PC1 was significantly more lytic than the reduced free peptide form (Figure 3) at both pH 5 and 7.5. Despite the same trend, this effect was less pronounced for PC2−pLLys conjugates, and no activity could be observed for PC4−pLLys conjugates (data not shown). The reason for this behavior of PC2 and PC4 is not known at present, but the formation of aggregates might play a role in the case of PC4; PC2, on the other hand, is negatively charged, and it is reasonable to assume that the positively charged pLLys may influence its leakage activity by neutralizing these charges and modulating the local pH. Poly (L-Lysine) alone does not result in the leakage of calcein from POPC LUVs (data not shown).

*Amino Acid Composition.* When studying the peptide sequences (Table 1) for their amino acid compositions, two trends are immediately apparent: the great number of prolines and the differences in amino acid composition reflective of the MLV lipid composition (Figure 4). Those peptides arising from screens against acidic ELM MLVs show a particularly high preponderance of histidines and a concurrent paucity of aromatic and hydrophobic amino acid residues, with the exception of methionine. In contrast, the sequences arising from phage screened against electroneutral POPC MLVs are highly aromatic.

To understand more quantitatively, the peptide profile of the POPC screen, which yielded the membrane-active peptides, the frequency of amino acid occurrence was compared against its counterpart frequencies in the parent Ph.D-12 library (Figure 4). This analysis was weighted for peptide occurrence, that is, the amino acid composition of each peptide sequence was multiplied with the frequency of occurrence of the clone. In the POPC MLV screen, from which the active peptides were identified, the aromatic amino acids are highly enriched (Tyr 1.6×, Phe 2.6×, Trp 4.8× enrichment above the parent library frequency). Not surprisingly, all titratable amino acids were enriched (aspartate 1.5×; glutamate 1.6× histidine 1.8×).

When comparing the individual sequences from the membrane-active peptides PC1, PC2, and PC4 to the nonactive peptides PC3, PC5, and PC6, discovered in the screen using POPC MLVs, it is striking that none of the active peptides have either an arginine or a lysine in their sequence. In contrast, tryptophan is highly enriched in the sequence of two of the three active peptides but completely absent from the inactive peptides. Among the active peptides, the sequences are quite distinct in their amino acid composition. The sequence of PC2 is dominated by aliphatics (33% not counting the *C*-terminal Cysteine) in addition to a partially aliphatic methionine and a phenylalanine. These hydrophobic amino acids and the two acidic glutamates arranged in a periodic manner are features reminiscent of helical viral fusion peptides. PC1, on the other hand, has three titratable amino acids and has a 2.8 higher content of aromatic amino acids and a 7.4 higher content of tryptophan than the parent library. The most intriguing sequence is the sequence of PC4. This peptide displays strongly pH-dependent lytic activity despite the lack of any titratable amino acids. Furthermore, all of its amino acids are overrepresented when compared to the parent library. Strikingly, tryptophan occurs 11.1× more often than by random chance.

It is tempting to speculate that the sequence diversity of the active peptides will be reflected in different mechanisms of membrane activity. PC4 in particular, lacking any titratable groups, promises to provide novel insights as to how peptides can induce pH-dependent permeabilization of liposomes.

*Peptide Structure.* Secondary structures are known to be important in peptide−membrane interactions. Amphipathic helices are seen in many lytic (*43*) and fusion peptides (*12*). Conversely, beta sheets can act on membranes (*44*) as beta aggregates (*45*, *46*), or they can insert into membranes as beta barrels (*47*). We therefore analyzed the secondary structure of our peptides by circular dichroism. We first chose TFE as a cosolvent because it serves as a model for the hydrophobic environment of the aliphatic core of membranes. In 50% TFE and in the concentration range tested (50−400 $\mu$M), SFP3, a peptide designed to maximize its helical content and hydrophobic moment (*41*), shows an $\alpha$-helical spectra with minima at 208 and 222 nm and small contributions from random coil or possibly a $3_{10}$ helix (*48*) (Figure 5). Two of our peptides, PC2, and, to a lesser extent, PC4 also show profiles consistent with $\alpha$-helical conformations. The above structures are present between 25 and 55 °C (data not shown). The partially helical conformation PC4 suggested by its CD spectrum is surprising given the preponderance of prolines and tryptophans. CD spectra of peptides, however, can be greatly influenced by aromatic amino acids (*49*). Hence, it is possible that this apparent partially helical profile is artifactual. Although PC1 shows pH-dependent lytic activity, notable structures were not observed under these solvent conditions. None of the other peptides showed any structure (data not shown).

To study the effect of pH and membranes on the structure of our peptides, we next determined the secondary structure of the three active peptides and the positive control SFP3 in aqueous buffered solutions at pH 5 and 7.5, both in the presence and absence of liposomes (Figure 6). The signal-to-noise ratio could not be optimized to obtain spectra for PC1 and PC4 under the range of conditions tested. PC2 showed a more prominent alpha-helical conformation at pH 5 than at 7.5, where the spectra suggest a stronger influence of a typical random coil. Upon addition of POPC SUVs, the characteristic alpha-helical minima at 222 nm became more prominent at both pH 5 and 7.5. SFP3 showed a similar pH-dependence with the peptide alone: deeper 222 nm well

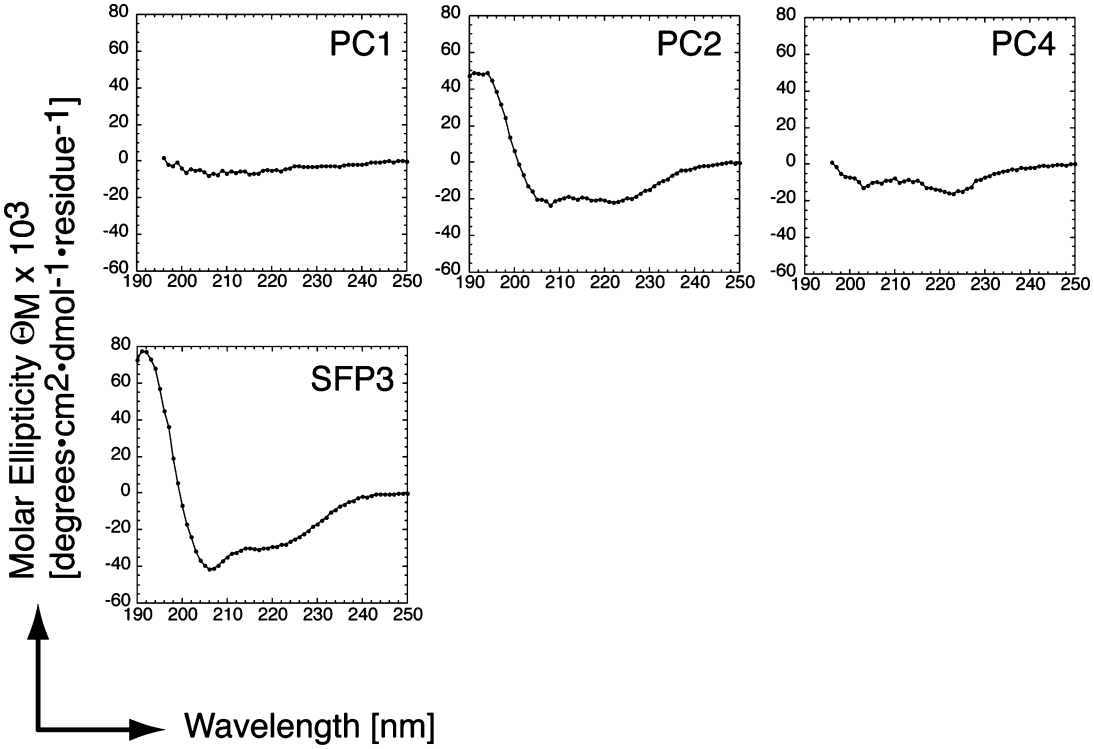


FIGURE 5: Secondary structure of peptides in TFE. Circular dichroism spectra were taken of peptides dissolved in TFE and measured at 50% TFE in water, 1 mM TCEP at 25 ± 2oC on a JASCO J-810 CD spectrometer. The spectra represented in molar ellipticity units did not change within the peptide concentrations range of 50−400 $\mu$M.

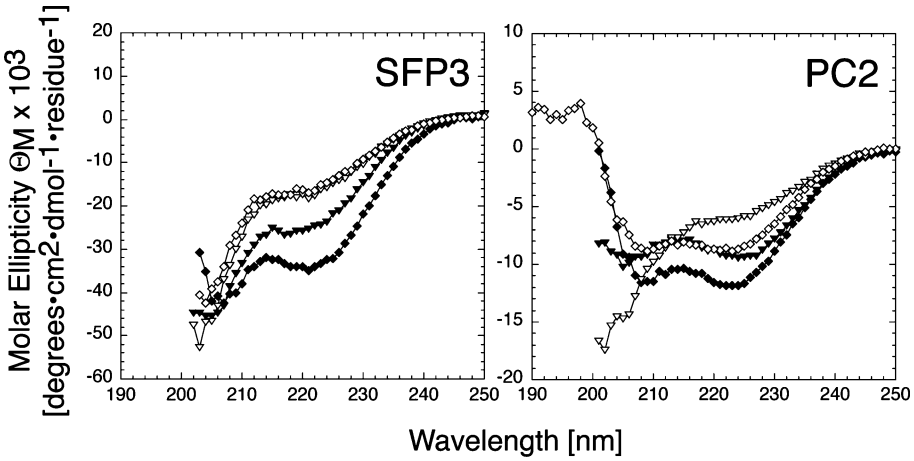


FIGURE 6: Effect of pH and lipids on peptide structure. The peptides were dissolved into 0.1% ammonia stock solution, from which dilutions were made. The final CD buffer was 0.01% ammonia, 2 mM citrate, 2 mM borate, 2 mM potassium phosphate with 10 mM sodium chloride, and 10 mM TCEP. The buffering components were used to adjust the solutions to the appropriate pH. The measurements were taken on a JASCO J-810 CD spectrometer at 25 ± 2 °C. The addition of lipids did not cause a disturbance in the baseline measurements (data not shown). Symbols: pH 5 (▼); pH 7.5 (▽); pH 5 with POPC SUVs (♦); pH 7.5 with POPC SUVs (◊). The peptide-to-lipid ratios were less than 0.6.

minima at pH 5 than at 7.5. In contrast to PC2, the addition of liposomes at pH 7.5 did not result in increased helicity for SFP3 as reflected in calcein leakage results (Table 3). Only in the presence of liposomes did the 222 nm well minima become more pronounced at pH 5. These trends of SFP3 are consistent with studies of the parent peptide GALA in the presence of lipids (*41*) and with its sister peptide SFP1 in aqueous solution without lipids (*40*).

Taken together with results from Table 3, the apparent rank order of lytic potencies does not seem to correlate with helicity, suggesting that additional parameters are influencing the lytic potential of these peptides. Nevertheless, the fact that both the lowering of pH as well as the addition of lipid membranes increase the helical profile of PC2 suggests a role of this structure in the pH-dependent membrane activity of this peptide. Future experiments, including additional spectroscopic methods and mutational analyses, will be needed to unravel the mechanisms of pH-dependent membrane activity of the diverse peptides discovered in this study.

## DISCUSSION

In this article, we set out to discover peptides that disturb membranes in a pH-dependent manner by screening an M13 12-mer filamentous phage library, Ph.D.-12, for pH-dependent liposome binding. Two different liposome types were used: one that represents the aliphatic lipid bilayer core,

POPC MLVs, and another mimicking the endosomal membrane, ELM MLVs. In this context, we have identified 19 distinct peptide sequences, of which three peptides, PC1, PC2, and PC4, are able to induce pH-dependent calcein leakage to an extent similar to that of the positive control peptides SFP3 and INF7* (Figure 2 and Table 3).

In contrast to the peptides identified from phage screens against receptors or antibodies (*50*), BLAST analysis showed that our panel of active peptides do not share significant homology with any proteins described. Instead, our peptides have varied sequences without an obvious consensus motif. This lack of a consensus sequence is not surprising because secondary (*12*) and multidimensional (*44*) homologies seem to be more important in defining membrane activity than their primary sequence.

On the amino acid level, compositions of the discovered peptides reflect the nature of the lipids against which the screen has been conducted, aromatic groups against isoelectric POPC liposomes, and basic and less hydrophobic residues against negatively charged ELM liposomes. We have also enriched for histidines, a titratable amino acid in the pH-range of the screen.

Against our expectations, aliphatic amino acids (with the exception of PC2) have not been enriched in our screens. Aromatics, however, were highly enriched in our POPC screen. Two of the membrane-active peptides, namely PC1 and PC4, have a striking number of tryptophans. In contrast, trypthophan occurred only once in the 13 sequences discovered in the ELM screen and was completely absent from all the inactive peptides isolated from the POPC screen (Table 1).

When peptide activity was determined in vitro using the calcein leakage assay (*26*), we found that PC1, PC2, and PC4 were active both on electroneutral POPC as well as negatively charged ELM liposomes. These results imply that the calcein leakage activity of peptides is not dependent on ionic interaction with the lipid headgroups, but is instead governed by the ability of the peptides to interact with the hydrophobic core of the lipid bilayer.

For PC1 and PC4, it is likely that the multiple tryptophans play an important role in this putative interfacial insertion into the bilayer. According to the Wimley−White interfacial hydrophobicity scale (*51*), aromatic and hydrophobic aliphatic residues (with the exception of valine) favor partitioning into a lipid bilayer (Figure 4). Tryptophan not only favors partitioning into bilayers more than aliphatics, but it is—unlike, for example, leucine—energetically undesirable to be located in the center of a transmembrane domain (*16*, *52*). The enrichment of tryptophans in the membrane-proximal domain has been implicated in the fusogenic activity of viral fusion proteins (*53*). The reason for the partial bilayer insertion of PC2, on the other hand, probably lies in its tendency to form an amphipathic helix as seen in classical viral fusion peptides (*54*). In a helical conformation, the acidic glutamates and the hydrophobic amino acids (leucine, isoleucine, and methionine) of PC2 lie on opposite faces of the helix.

Another factor that can influence both the membrane activity of peptides as well as the angle of peptide insertion into membranes is peptide length. Peptide length is often cited as a reason for diminished membrane activity of shorter peptides. Although there are 6-mers (*55*) that have been shown to be membrane-active and 8 amino acid peptides are reported to interact stably with membranes (*56*), the membrane-active peptides studied in most detail are helices of a length of approximately 20 amino acids. One particularly well-studied peptide is the *N*-terminus of the influenza fusion protein hemagglutinin. In this model, using a host−guest system, increased peptide length increases both the depth and angle of membrane insertion as well as contents leakage from red blood cells (*57*). Given this information, it is remarkable that the 13 amino acid-long peptides in our study enable contents leakage to an extent similar to that of the 24 amino acid-long influenza fusion peptide analogue INF7* (Table 3), which has been optimized for its lytic activity (*28*).

Together, these results suggest that the propensity of the membrane-active peptides to insert shallowly into the membrane is important for their lytic activity. The ability to penetrate deep into the hydrophobic core, however, may be less significant. The data are indeed consistent with a model in which a shallow interaction with the hydrophobic core of a bilayer is sufficient to induce content leakage.

Most membrane-interacting synthetic peptides are more active as dimers (*58*, *59*) and oligomers (*60*) or when anchored to a membrane (*40*). This principle also holds true for two of our leakage-active peptides, PC2 and, especially, PC1 (Figure 3). PC1 conjugated to poly(L-Lysine) by disulfide bonds, a multimeric presentation, is considerably more active in the calcein-leakage assay than when the peptide was released from the oligomer in the presence of 1 mM DTT.

As stated in the introduction, membrane binding is obligatory, though not necessarily sufficient, for a peptide to be membrane-active. True to this prediction, the peptides identified in our screen that lost the ability to bind stably to membranes are not lytic. The fact that in the context of the phage, the peptides are both *C*-terminally anchored to a protein as well as being displayed in a pentameric form likely influences their ability to interact with membranes. Especially, because oligomeric presentation of the peptides almost certainly increases avidity, it is not surprising that some peptides, PC3, PC5, and PC6 as well as ELM1, ELM2, and ELM3, lost the ability to bind stably to liposomes in their monomeric form.

PC1 binds to both POPC and ELM liposomes. This is not unexpected because, as stated above, the interaction of PC1 with membranes is less likely to be influenced by the surface charge but more likely by the insertion of the peptide into the aliphatic core of the bilayer. Interestingly, the membrane-active peptides PC1, PC2, and PC4 bind to MLVs at both pHs. This appears to conflict both with the phage screen, which was based on the elution of the phages at pH 7.5, as well as the calcein leakage results. The simplest explanation for this behavior lies in the different natures of the liposome-binding assay and the phage screen and calcein-leakage assay. In the phage screen, the eluted phages are amplified in each round of screening. Even if only a small amount of bound phage is eluted at pH 7.5, the bulk of the phage remaining bound to MLVs, it will be amplified and thus recovered in the screen. The liposome-binding assay, however, measures the binding of the bulk of peptides.

Despite the pH-independent binding of the peptides to MLVs, the lytic activity of all active peptides is strongly pH-dependent. Apparently, the lytic activity of our peptides is influenced by additional factors such as pH-dependent

structural changes and not just the binding to liposomes. Alternatively, the reason for the difference between binding and lytic activity might lie in the different peptide and lipid concentrations used in the two assays. Because of the detection limit in the liposome binding assay, both the lipid and the peptide concentrations were substantially higher in the binding than in the leakage assay.

The secondary structure of peptides has been instrumental in further understanding the interaction of peptides with membranes. Many of the membrane-interacting components of viruses form amphipathic helices (*12*). In line with these observations, we find that two of our peptides, PC2 and PC4, despite their short length, show helical propensities in 50% TFE (Figure 5). Because of the highly aromatic amino acid composition of PC4, the helical structure of this peptide must, however, be confirmed by other methods (*49*). The helicity of PC2 in aqueous solution shows a pH- and lipid-dependent increase, reminiscent of the conformational change and the resulting deeper membrane insertion of influenza fusion domain at acidic pH (*61*). Thus, a model in which this change in helicity plays a role in the lytic activity of PC2 is particularly attractive.

The fact that PC4 tends to aggregate in solution might also play an important role in the leakage potential of this peptide. Interestingly, the aggregation of PC4 in solution was not strongly dependent on pH, in contrast to the pH-dependent leakage induced by PC4. This disparity suggests that differences exist in peptide organization in the absence or presence of membranes. These results are consistent with other studies showing that peptide assembly on membrane templates and aggregation has an important role in membrane activity (*57*, *59*).

PC4 is of further interest because it possesses pH-dependent lytic activity in the absence of any titratable groups. One possible reason for the pH-dependency of PC4 is the presence of two prolines. Prolines can confer pH sensitivity by isomerizing in a pH-dependent manner (*62*). The possible importance of prolines for the pH-dependent lytic activity of PC4 is highlighted by the fact that the probability of the double prolines at position 9 and 10 to occur by random chance in our screen is less than $10^{-7}$ (Materials and Methods). This indicates that these prolines are a result of the selective pressure in this screen for pH-dependent phage binding to the membranes. These findings resonate with the fact that centrally located prolines (*63*) and their ability to change between secondary structures (*55*, *64*, *65*) play an integral role in pH-dependent membrane destabilization induced by other peptides.

Our work demonstrates that peptides that are membrane-active in a pH-dependent fashion can be identified by phage display. The study also demonstrates that the choice of lipids used in the screen is important in selecting for activity. When the screen is performed with electroneutral PC liposomes that mimic the aliphatic core, 50% of the sequences discovered on the screen produced pH-dependent lytic peptides. Furthermore, membrane-active peptides, as opposed to their inactive counterparts, contain a remarkably high content of tryptophan, reminiscent of antimicrobial peptides (*66*), suggesting a crucial role of this amino acid in the lytic behavior of these peptides.

Future studies aimed at deciphering the mechanism of membrane activity will help us to put these newly identified peptides into the context of both naturally occurring as well as synthetic lytic peptides. The present approach may also open new avenues to gain a deeper understanding of peptide−lipid interactions and their role in cell biological and pathological processes, with the potential of yielding new strategies for therapeutic applications.

## ACKNOWLEDGMENT

We acknowledge the expert technical assistance of C. Cruickshank during the initial phase of this project. We also thank J. Carlson, A. Kentsis, and the Department of Structural Biology at Mount Sinai School of Medicine for their assistance in the use of the JASCO J-810 CD spectrometer and K. Senn, L. Gigout, R. Fransis, F. Paumet, M. Linden, A. Thomas, and R. Brasseur for insightful discussions.

## SUPPORTING INFORMATION AVAILABLE

The probabilities of a peptide sequence's random occurrence in the parent library were calculated using INFO of the RELIC suite of programs (*30*) to determine if multiply occurring peptides were an inherent result of incomplete sequence representation or positional amino acid biases dictated by M13 phage biology of the parent Ph.D.-12 library (*39*). This material is available free of charge via the Internet at http://pubs.acs.org.

## REFERENCES

1. Cho, W., and Stahelin, R. V. (2005) Membrane-protein interactions in cell signaling and membrane trafficking, *Annu. Rev. Biophys. Biomol. Struct. 34*, 119−151.
2. Holthuis, J. C., and Levine, T. P. (2005) Lipid traffic: floppy drives and a superhighway, *Nat. Rev. Mol. Cell Biol. 6*, 209−220.
3. Pelchen-Matthews, A., Raposo, G., and Marsh, M. (2004) Endosomes, exosomes and Trojan viruses, *Trends Microbiol. 12*, 310−316.
4. Byland, R., and Marsh, M. (2005) Trafficking of viral membrane proteins, *Curr. Top. Microbiol. Immunol. 285*, 219−254.
5. Tamm, L. K., Crane, J., and Kiessling, V. (2003) Membrane fusion: a structural perspective on the interplay of lipids and proteins, *Curr. Opin. Struct. Biol. 13*, 453−466.
6. Pécheur, E. I., Sainte-Marie, J., Bienvenüe, A., and Hoekstra, D. (1999) Peptides and membrane fusion: towards an understanding of the molecular mechanism of protein-induced fusion, *J. Membr. Biol. 167*, 1−17.
7. Simoes, S., Slepushkin, V., Gaspar, R., de Lima, M. C., and Duzgunes, N. (1998) Gene delivery by negatively charged ternary complexes of DNA, cationic liposomes and transferrin or fusigenic peptides, *Gene Ther. 5*, 955−964.
8. Martin, I., and Ruysschaert, J. M. (2000) Common properties of fusion peptides from diverse systems, *Biosci. Rep. 20*, 483−500.
9. Pouny, Y., Rapaport, D., Mor, A., Nicolas, P., and Shai, Y. (1992) Interaction of antimicrobial dermaseptin and its fluorescently labeled analogues with phospholipid membranes, *Biochemistry 31*, 12416−12423.
10. Shai, Y. (1999) Mechanism of the binding, insertion and destabilization of phospholipid bilayer membranes by alpha-helical antimicrobial and cell nonselective membrane-lytic peptides, *Biochim. Biophys. Acta 1462*, 55−70.
11. Rafalski, M., Ortiz, A., Rockwell, A., van Ginkel, L. C., Lear, J. D., DeGrado, W. F., and Wilschut, J. (1991) Membrane fusion activity of the influenza virus hemagglutinin: interaction of HA2 *N*-terminal peptides with phospholipid vesicles, *Biochemistry 30*, 10211−10220.
12. Epand, R. M. (2003) Fusion peptides and the mechanism of viral fusion, *Biochim. Biophys. Acta 1614*, 116−121.
13. Del Angel, V. D., Dupuis, F., Mornon, J. P., and Callebaut, I. (2002) Viral fusion peptides and identification of membrane-interacting segments, *Biochem. Biophys. Res. Commun. 293*, 1153−1160.

14. Brunner, J., and Tsururud. (1993) Fusion-protein membrane interactions as studied by hydrophobic photolabeling, in *Viral Fusion Mechanisms* (Bentz, J., Ed.), pp 67−88, CRC Press, Boca Raton, FL.
15. Hristova, K., and White, S. H. (2005) An experiment-based algorithm for predicting the partitioning of unfolded peptides into phosphatidylcholine bilayer interfaces, *Biochemistry 44*, 12614−12619.
16. Hessa, T., Kim, H., Bihlmaier, K., Lundin, C., Boekel, J., Andersson, H., Nilsson, I., White, S. H., and von Heijne, G. (2005) Recognition of transmembrane helices by the endoplasmic reticulum translocon, *Nature 433*, 377−381.
17. Lins, L., Charloteaux, B., Heinen, C., Thomas, A., and Brasseur, R. (2006) "De novo" design of peptides with specific lipid-binding properties, *Biophys. J. 90*, 470−479.
18. Szardenings, M. (2003) Phage display of random peptide libraries: applications, limits, and potential, *J. Recept. Signal Transduction Res. 23*, 307−349.
19. Wimley, W. C., and White, S. H. (2000) Designing transmembrane alpha-helices that insert spontaneously, *Biochemistry 39*, 4432−4442.
20. Li, W., Nicol, F., and Szoka, F. C., Jr. (2004) GALA: a designed synthetic pH-responsive amphipathic peptide with applications in drug and gene delivery, *Adv. Drug Delivery Rev. 56*, 967−985.
21. Hong, S. Y., Oh, J. E., Kwon, M., Choi, M. J., Lee, J. H., Lee, B. L., Moon, H. M., and Lee, K. H. (1998) Identification and characterization of novel antimicrobial decapeptides generated by combinatorial chemistry, *Antimicrob. Agents Chemother. 42*, 2534−2541.
22. Fisher, L. E., and Engelman, D. M. (2001) High-yield synthesis and purification of an alpha-helical transmembrane domain, *Anal. Biochem. 293*, 102−108.
23. Di Simone, C., Zandonatti, M. A., and Buchmeier, M. J. (1994) Acidic pH triggers LCMV membrane fusion activity and conformational change in the glycoprotein spike, *Virology 198*, 455−465.
24. Erbacher, P., Remy, J. S., and Behr, J. P. (1999) Gene transfer with synthetic virus-like particles via the integrin-mediated endocytosis pathway, *Gene Ther. 6*, 138−145.
25. MacDonald, R. C., Macdonald, R. I., Menco, B. P. M., Takeshita, K., Subbarao, N. K., and Hu, L.-R. (1991) Small-volume extrusion apparatus for preparation of large, unilamellar vesicles, *Biochim. Biophpys. Acta 1061*, 297−303.
26. Duzgunes, N., Straubinger, R. M., Baldwin, P. A., Friend, D. S., and Papahadjopoulos, D. (1985) Proton-induced fusion of oleic acid-phosphatidylethanolamine liposomes, *Biochemistry 24*, 3091−3098.
27. Moore, S., and Stein, W. H. (1954) A modified Ninhydrin reagent for the photometric determination of amino acids and related compounds, *J. Biol. Chem. 211*, 907−913.
28. Plank, C., Oberhauser, B., Mechtler, K., Koch, C., and Wagner, E. (1994) The influence of endosome-disruptive peptides on gene transfer using synthetic virus-like gene transfer systems, *J. Biol. Chem. 269*, 12918−12924.
29. Deleted in proof.
30. Mandava, S., Makowski, L., Devarapalli, S., Uzubell, J., and Rodi, D. J. (2004) RELIC- -a bioinformatics server for combinatorial peptide analysis and identification of protein−ligand interaction sites, *Proteomics 4*, 1439−60.
31. Bailey, T. L., and Gribskov, M. (1998) Combining evidence using p-values: application to sequence homology searches, *Bioinformatics 14*, 48−54.
32. Stein, B. S., Gowda, S. D., Lifson, J. D., Penhallow, R. C., Bensch, K. G., and Engleman, E. G. (1987) pH-independent HIV entry into CD4-positive T cells via virus envelope fusion to the plasma membrane, *Cell 49*, 659−668.
33. Stegmann, T., Morselt, H. W., Scholma, J., and Wilschut, J. (1987) Fusion of influenza virus in an intracellular acidic compartment measured by fluorescence dequenching, *Biochim. Biophys. Acta 904*, 165−170.
34. Wiethoff, C. M., Wodrich, H., Gerace, L., and Nemerow, G. R. (2005) Adenovirus protein VI mediates membrane disruption following capsid disassembly, *J. Virol. 79*, 1992−2000.
35. Jardetzky, T. S., and Lamb, R. A. (2004) Virology: a class act, *Nature 427*, 307−308.
36. Duzgunes, N., and Gambale, F. (1988) Membrane action of synthetic N-terminal peptides of influenza virus hemagglutinin and its mutants, *FEBS Lett. 227*, 110−114.
37. Schlegel, R., and Wade, M. (1984) A synthetic peptide corresponding to the NH2 terminus of vesicular stomatitis virus glycoprotein is a pH-dependent hemolysin, *J. Biol. Chem. 259*, 4691−4694.
38. Hewat, E. A., and Blaas, D. (2004) Cryoelectron microscopy analysis of the structural changes associated with human rhinovirus type 14 uncoating, *J. Virol. 78*, 2935−2942.
39. Rodi, D. J., Soares, A. S., and Makowski, L. (2002) Quantitative assessment of peptide sequence diversity in M13 combinatorial peptide phage display libraries, *J. Mol. Biol. 322*, 1039−1052.
40. Puyal, C., Maurin, L., Miquel, G., Bienvenue, A., and Philippot, J. (1994) Design of a short membrane-destabilizing peptide covalently bound to liposomes, *Biochim. Biophys. Acta 1195*, 259−266.
41. Subbarao, N. K., Parente, R. A., Szoka, F. C., Jr., Nadasdi, L., and Pongracz, K. (1987) pH-dependent bilayer destabilization by an amphipathic peptide, *Biochemistry 26*, 2964−2972.
42. Hernandez, L. D., Hoffman, L. R., Wolfsberg, T. G., and White, J. M. (1996) Virus-cell and cell-cell fusion, *Annu. Rev. Cell Dev. Biol. 12*, 627−661.
43. Zelezetsky, I., Pacor, S., Pag, U., Papo, N., Shai, Y., Sahl, H. G., and Tossi, A. (2005) Controlled alteration of the shape and conformational stability of alpha-helical cell-lytic peptides: effect on mode of action and cell specificity, *Biochem. J.*
44. Rausch, J. M., Marks, J. R., and Wimley, W. C. (2005) Rational combinatorial design of pore-forming {beta}-sheet peptides, *Proc. Natl. Acad. Sci. U.S.A. 102*, 10511−10515.
45. Kremer, J. J., Pallitto, M. M., Sklansky, D. J., and Murphy, R. M. (2000) Correlation of beta-amyloid aggregate size and hydrophobicity with decreased bilayer fluidity of model membranes, *Biochemistry 39*, 10309−10318.
46. Bokvist, M., Lindstrom, F., Watts, A., and Grobner, G. (2004) Two types of Alzheimer's beta-amyloid (1−40) peptide membrane interactions: aggregation preventing transmembrane anchoring versus accelerated surface fibril formation, *J. Mol. Biol. 335*, 1039−1049.
47. Wimley, W. C. (2003) The versatile beta-barrel membrane protein, *Curr. Opin. Struct. Biol. 13*, 404−411.
48. Biron, Z., Khare, S., Samson, A. O., Hayek, Y., Naider, F., and Anglister, J. (2002) A monomeric 3(10)-helix is formed in water by a 13-residue peptide representing the neutralizing determinant of HIV-1 on gp41, *Biochemistry 41*, 12687−12696.
49. Vuilleumier, S., Sancho, J., Loewenthal, R., and Fersht, A. R. (1993) Circular dichroism studies of barnase and its mutants: characterization of the contribution of aromatic side chains, *Biochemistry 32*, 10303−10313.
50. Beckmann, C., Brittnacher, M., Ernst, R., Mayer-Hamblett, N., Miller, S. I., and Burns, J. L. (2005) Use of phage display to identify potential *Pseudomonas aeruginosa* gene products relevant to early cystic fibrosis airway infections, *Infect. Immun. 73*, 444−452.
51. Wimley, W. C., and White, S. H. (1996) Experimentally determined hydrophobicity scale for proteins at membrane interfaces, *Nat. Struct. Biol. 3*, 842−848.
52. Kamimori, H., Blazyk, J., and Aguilar, M. I. (2005) Lipid membrane-binding properties of tryptophan analogues of linear amphipathic beta-sheet cationic antimicrobial peptides using surface plasmon resonance, *Biol. Pharm. Bull. 28*, 148−150.
53. Sainz, B., Jr., Rausch, J. M., Gallaher, W. R., Garry, R. F., and Wimley, W. C. (2005) The aromatic domain of the coronavirus class I viral fusion protein induces membrane permeabilization: putative role during viral entry, *Biochemistry 44*, 947−958.
54. Takahashi, S. (1990) Conformation of membrane fusion-active 20-residue peptides with or without lipid bilayers. Implication of alpha-helix formation for membrane fusion, *Biochemistry 29*, 6257−6264.
55. Pecheur, E. I., Martin, I., Bienvenue, A., Ruysschaert, J. M., and Hoekstra, D. (2000) Protein-induced fusion can be modulated by target membrane lipids through a structural switch at the level of the fusion peptide, *J. Biol. Chem. 275*, 3936−3942.
56. McLean, L. R., Hagaman, K. A., Owen, T. J., and Krstenansky, J. L. (1991) Minimal peptide length for interaction of amphipathic alpha-helical peptides with phosphatidylcholine liposomes, *Biochemistry 30*, 31−37.
57. Han, X., and Tamm, L. K. (2000) A host−guest system to study structure−function relationships of membrane fusion peptides, *Proc. Natl. Acad. Sci. U.S.A. 97*, 13097−13102.

58. Kovacs, F., Quine, J., and Cross, T. A. (1999) Validation of the single-stranded channel conformation of gramicidin A by solid-state NMR, *Proc. Natl. Acad. Sci. U.S.A. 96*, 7910−7915.
59. Haas, D. H., and Murphy, R. M. (2004) Templated assembly of the pH-sensitive membrane-lytic peptide GALA, *J. Pept. Res. 63*, 451−459.
60. Yang, R., Prorok, M., Castellino, F. J., and Weliky, D. P. (2004) A trimeric HIV-1 fusion peptide construct which does not self-associate in aqueous solution and which has 15-fold higher membrane fusion rate, *J. Am. Chem. Soc. 126*, 14722−14723.
61. Han, X., Bushweller, J. H., Cafiso, D. S., and Tamm, L. K. (2001) Membrane structure and fusion-triggering conformational change of the fusion domain from influenza hemagglutinin, *Nat. Struct. Biol. 8*, 715−720.
62. Brasseur, R., Cabiaux, V., Falmagne, P., and Ruysschaert, J. M. (1986) pH dependent insertion of a diphtheria toxin B fragment peptide into the lipid membrane: a conformational analysis, *Biochem. Biophys. Res. Commun. 136*, 160−168.
63. Afonin, S., Durr, U. H., Glaser, R. W., and Ulrich, A. S. (2004) 'Boomerang'-like insertion of a fusogenic peptide in a lipid membrane revealed by solid-state 19F NMR, *Magn. Reson. Chem. 42*, 195−203.
64. Delos, S. E., Gilbert, J. M., and White, J. M. (2000) The central proline of an internal viral fusion peptide serves two important roles, *J. Virol. 74*, 1686−1693.
65. Hofmann, M. W., Weise, K., Ollesch, J., Agrawal, P., Stalz, H., Stelzer, W., Hulsbergen, F., de Groot, H., Gerwert, K., Reed, J., and Langosch, D. (2004) De novo design of conformationally flexible transmembrane peptides driving membrane fusion, *Proc. Natl. Acad. Sci. U.S.A. 101*, 14776−14781.
66. Hsu, C. H., Chen, C., Jou, M. L., Lee, A. Y., Lin, Y. C., Yu, Y. P., Huang, W. T., and Wu, S. H. (2005) Structural and DNA-binding studies on the bovine antimicrobial peptide, indolicidin: evidence for multiple conformations involved in binding to membranes and DNA, *Nucleic Acids Res. 33*, 4053−4064.

BI052488S